Electrical Power and Energy Systems 78 (2016) 700–714

Contents lists available at ScienceDirect

Electrical Power and Energy Systems

journal homepage: www.elsevier.com/locate/ijepes

Solution of optimal power flow with FACTS devices using a novel oppositional krill herd algorithm

Aparajita Mukherjee, V. Mukherjee *

Department of Electrical Engineering, Indian School of Mines, Dhanbad, Jharkhand, India

ARTICLE INFO

Article history:
Received 30 October 2014
Received in revised form 30 November 2015
Accepted 4 December 2015
Available online 29 December 2015

Keywords:
FACTS devices
Krill herd algorithm
Opposite number
Optimal power flow
Optimization

ABSTRACT

Krill herd algorithm (KHA) is a novel meta-heuristic approach that is influenced from the herding behaviour of the krill swarms searching for food or communication with each other. The proposed opposition based KHA (OKHA) is intended here, for solving the optimal power flow (OPF) problem of power system, incorporating flexible AC transmission systems (FACTS) devices, namely, thyristor controlled series capacitor and thyristor controlled phase shifter. In the proposed OKHA, the concept of opposition based population initialization and opposition based generation jumping are employed in the basic KHA to enhance its computational speed and convergence profile. The potential of the proposed OKHA is assessed, successfully, on modified IEEE-30 bus and IEEE-57 bus test power systems. The four different objective functions are formulated here that reflects the minimization of fuel cost, active power transmission loss, emission and combined economic and environmental cost, separately. Simulation results, presented in this paper, indicate that the proposed approach yields superior solution over the other popular methods surfaced in the recent state-of-the-art literature including basic KHA and also show its effectiveness for the solution of OPF problem of power system equipped with FACTS devices.

© 2015 Elsevier Ltd. All rights reserved.

Introduction

Optimal power flow (OPF) is a useful tool in modern energy management system. It plays an important role for secure operation of power system operation, control and planning. The preliminary goal of generic OPF is to minimize the total production cost of the entire system for fulfilment of the load demand of a particular power system by maintaining the security of the system operation [1,2]. At steady state condition, each device in the power system should be within its desired operating range. These include minimum and maximum limits of (a) generators' real and reactive power outputs, (b) load voltage magnitudes of each bus in the network, (c) apparent power flows of power transmission lines, (d) transformers' tap setting and (e) reactive power injection. This method has been studied, rigorously, over the past few decades and it has been solved, successfully, by a wide variation of conventional optimization techniques such as Newton method [3], linear programming, dynamic programming and interior point method [4]. Many evolutionary optimization techniques such as genetic algorithm (GA) [5], evolutionary programming [6], artificial bee colony, bacteria foraging optimization, gravitational search algorithm [7] have been proposed in the literature assuming the OPF problem as continuous, differential and having monotonically increasing cost function. However, practical systems consider higher order non-linearity effect of thermal generating units and discontinuities due to valve point loading effect. Therefore, new optimization methods are required to solve such difficulties. Some of these population based methods are tabu search [8], particle swarm optimization (PSO) [9], biogeography based optimization (BBO) [10–12], etc. These methods can solve non-convex, non-smooth and non-differentiable optimization problems efficiently and effectively.

But in the deregulated power industry, flexible AC transmission systems (FACTS) are being extensively used in the recent days to increase the power transfer capability of long transmission line as well as to improve the system stability. These devices are capable to control current, voltage, impedance and phase angle of the transmission system for increasing the system stability, power factor correction, loss minimization and most importantly management of active and reactive power flow and voltage profile [13]. Hence, the conventional OPF problem, incorporated with FACTS devices [14,15], has opened new opportunities for controlling the real and reactive power flow and various optimization techniques like hybrid GA [16], simulated annealing [17], real coded GA [14], differential evolution (DE) [14], dynamic strategy based fast decomposed GA [18], craziness PSO and turbulent crazy PSO [19], PSO with

* Corresponding author. Tel.: +91 326 2235644.
E-mail addresses: mukherjeeaparajita29@gmail.com (A. Mukherjee), vivek_agamani@yahoo.com (V. Mukherjee).

http://dx.doi.org/10.1016/j.ijepes.2015.12.001
0142-0615/© 2015 Elsevier Ltd. All rights reserved.

Nomenclature

a_p, b_p, c_p	fuel cost coefficients of the pth generator
d_p, e_p	fuel cost coefficients with valve point loading effect of the pth generator
$E(P_g)$	total emission
F_C	total fuel cost of generating units
$g(\boldsymbol{u}, \boldsymbol{v})$	set of equality constraints
G_k	conductance of the kth line connected between the pth and the qth buses
G_{pq}, B_{pq}	conductance and susceptance between bus p and q, respectively
$h(\boldsymbol{u}, \boldsymbol{v})$	set of inequality constraints
N_B	total number of buses
N_C	number of capacitor banks
N_L	number of transmission lines
N_{PQ}	number of load buses
N_{PV}	number of generator buses
N_T	number of tap setting transformer branches
N_{TCPS}	number of TCPS devices installed in the test power system
N_{TCSC}	number of TCSC devices installed in the test power system
$\boldsymbol{of}$	objective function to be minimized
$OF(FU, E)$	combined economic environmental cost
P_{Gp}, Q_{Gp}	active and reactive power generations of the pth bus, respectively
$P_{Gp}^{min}, P_{Gp}^{max}$	minimum and maximum limits of active power of the pth generating unit, respectively
P_{Loss}	total power loss
P_{Lp}, Q_{Lp}	active and reactive power demands of the pth bus, respectively
P_{pk}, Q_{pk}	injected real and reactive powers of TCPS at the pth bus, respectively
P_{pq}, Q_{pq}	active and reactive power flows from pth to qth bus, respectively
P_{ps}, Q_{ps}	injected real and reactive powers at bus p due to TCPS, respectively
P_{qs}, Q_{qs}	injected real and reactive powers at bus q due to TCPS, respectively
$Q_{Cp}^{min}, Q_{Cp}^{max}$	minimum and maximum VAR injection limits of pth shunt capacitor, respectively
$Q_{Gp}^{min}, Q_{Gp}^{max}$	minimum and maximum limits of reactive power of the pth generating unit, respectively
R_{pq}, X_{pq}	resistance and reactance of the transmission line, respectively
S_{Lp}	apparent power flow of the pth branch
S_{Lp}^{max}	maximum apparent power flow limit of pth branch
T_p^{min}, T_p^{max}	minimum and maximum tap setting limits of pth transformer, respectively
$\boldsymbol{u}$	vector of dependent variables
$\boldsymbol{v}$	vector of independent variables
$V_{Lp}^{min}, V_{Lp}^{max}$	minimum and maximum load voltage of the pth load bus, respectively
V_p, V_q	voltage magnitudes at bus p and q, respectively
X_C	reactance of TCSC placed in the transmission line connected between pth and qth bus
$X_{Tp}^{min}, X_{Tp}^{max}$	minimum and maximum reactance of the pth TCSC, respectively
Y_{pq}	the total admittance of the transmission line connected between pth and qth bus
$\alpha_p, \beta_p, \gamma_p, \eta_p, \lambda_p$	emission coefficients of the pth generator
$\phi_{Tp}^{min}, \phi_{Tp}^{max}$	minimum and maximum phase shift angle of the pth TCPS, respectively
θ_{pq}	admittance angle of the transmission line connected between pth and qth bus

ageing leader and challengers (ALC-PSO) [20] have been employed for solving this type of OPF problem of power system.

KHA [21], a new bio-inspired and swarm intelligent approach, has been proposed by Gandomi and Alavi for global optimization problem in 2012. This technique is based upon the analogy of simulating the herding behaviour of krill swarms in nature. The position for each individual krill is determined from three different actions *viz.* (a) motion induced by other krill, (b) foraging activity and (c) random diffusion. Recently, KHA has been used in some areas of research interest like multimodal numerical optimization problems [22], portfolio optimization problems [23], combined heat and power dispatch problem [24], structural optimization problems [25] and optimum design of truss structures [26]. A few variants of hybrid KHA have been proposed in the literature like chaos theory based KHA for solving the benchmark functions problem [27], optimal reactive power dispatch problems [28], fuzzy KHA (that uses fuzzy system as parameter tuner) for benchmark test function optimization [29], stud KHA (that introduces stud selection and crossover operator for numerical optimization process) [30] and DE assisted KHA for economic load dispatch problem of power system [31]. Thus, literature survey reveals that this algorithm or its any variant are yet to apply in the OPF problem of power system equipped with FACTS devices. Thus, the motivation of the proposed work gets developed.

In the present work, the concept of opposition based learning (OBL) [32] and opposition based generation jumping are combined with the basic KHA for achieving enhanced computational speed and improved convergence speed. OBL is proved in the literature to be an effective solution technique applied with various optimization approaches [33–35]. Thus, this paper proposes a novel optimization technique termed as oppositional KHA (OKHA) for the solution of OPF problem of power system equipped with FACTS devices.

In this article, two FACTS devices, namely, thyristor controlled series capacitor (TCSC) and thyristor controlled phase shifter (TCPS) are considered for the solution of OPF problem of modified IEEE-30 bus and IEEE-57 bus test power systems. These two FACTS devices are considered to be located at fixed strategic locations of the considered power networks. The proposed OKHA aims to determine the optimal settings of variables with four different objectives, separately, such as minimization of (a) fuel cost (with and without considering valve point effect), (b) active power transmission loss, (c) emission and (d) combined fuel cost and emission while maintaining all the equality and inequality constraints as well as physical limits of FACTS devices. The results obtained are compared with those reported in the recent state-of-the-art literature.

The rest of the paper is organised as follows: Section 'Steady state models of FACTS devices' represents the modelling part of FACTS devices. Problem formulation part is presented in section 'Mathematical problem formulation'. 'KHA' portion describes the basic KHA. 'OKHA' illustrates the proposed OKHA. The implementation part of the proposed algorithm is described in 'Implementation of OKHA for OPF problem with FACTS'. Simulation results are presented and discussed in section 'Simulation results and discussion'. Finally, conclusions of the present work along with scope of

future work are presented in 'Conclusion and scope of future work' section.

Steady state models of FACTS devices

Modelling of TCSC

The effect of TCSC on a power system network may be represented by a controllable reactance which is inserted in series with the related transmission line. The static model of the network with TCSC connected between the pth and the qth bus is shown in Fig. 1 [13,36]. The corresponding power flow equations of the line having TCSC may be derived as follows [15,20]:

$$P_{pq} = V_p^2 G_{pq} - V_p V_q G_{pq} \cos(\delta_p - \delta_q) - V_p V_q B_{pq} \sin(\delta_p - \delta_q) \quad (1)$$

$$Q_{pq} = -V_p^2 B_{pq} - V_p V_q G_{pq} \sin(\delta_p - \delta_q) + V_p V_q B_{pq} \cos(\delta_p - \delta_q) \quad (2)$$

$$P_{qp} = V_q^2 G_{pq} - V_p V_q G_{pq} \cos(\delta_p - \delta_q) + V_p V_q B_{pq} \sin(\delta_p - \delta_q) \quad (3)$$

$$Q_{qp} = -V_q^2 B_{pq} + V_p V_q G_{pq} \sin(\delta_p - \delta_q) + V_p V_q B_{pq} \cos(\delta_p - \delta_q) \quad (4)$$

where

$$\text{Conductance of transmission line } (G_{pq}) = \frac{R_{pq}}{R_{pq}^2 + (X_{pq} - X_C)^2} \quad (5)$$

$$\text{Susceptance of transmission line } (B_{pq}) = -\frac{X_{pq} - X_C}{R_{pq}^2 + (X_{pq} - X_C)^2} \quad (6)$$

P_{pq}, Q_{pq} are the real and reactive power flows between the pth and the qth bus, respectively; V_p, V_q are the voltage magnitudes at bus p and q, respectively; G_{pq}, B_{pq} are the conductance and susceptance between bus p and q, respectively; δ_p, δ_q are the voltage angles at the pth and the qth bus, respectively; R_{pq}, X_{pq} are the resistance and reactance of the transmission line, respectively and X_C represents reactance of TCSC placed in the transmission line connected between pth and qth bus.

Modelling of TCPS

TCPS may be modelled by a phase shifting transformer having a complex tapping ratio of $1:1\angle\phi$ and series admittance of $Y_{pq}(= G_{pq} - sqrt(-1)B_{pq})$, connected between pth and qth bus as shown in Fig. 2. [13,36]. The corresponding power flow equations of the line may be expressed as follows [15,20]:

$$P_{pq} = \frac{V_p^2 G_{pq}}{\cos^2\phi} - \frac{V_p V_q}{\cos\phi}[G_{pq}\cos(\delta_p - \delta_q + \phi) + B_{pq}\sin(\delta_p - \delta_q + \phi)] \quad (7)$$

$$Q_{pq} = -\frac{V_p^2 B_{pq}}{\cos^2\phi} - \frac{V_p V_q}{\cos\phi}[G_{pq}\sin(\delta_p - \delta_q + \phi) - B_{pq}\cos(\delta_p - \delta_q + \phi)] \quad (8)$$

$$P_{qp} = V_q^2 G_{pq} - \frac{V_p V_q}{\cos\phi}[G_{pq}\cos(\delta_p - \delta_q + \phi) - B_{pq}\sin(\delta_p - \delta_q + \phi)] \quad (9)$$

$$Q_{qp} = -V_q^2 B_{pq} + \frac{V_p V_q}{\cos\phi}[G_{pq}\sin(\delta_p - \delta_q + \phi) + B_{pq}\cos(\delta_p - \delta_q + \phi)] \quad (10)$$

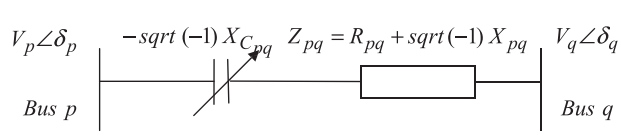

Fig. 1. Circuit model of TCSC connected between pth bus and qth bus.

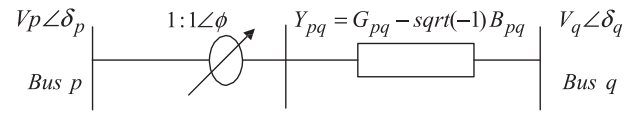

Fig. 2. Circuit model of TCPS connected between pth and qth bus.

The static model of TCPS is shown in Fig. 3. [13,36]. The injected active and reactive powers of TCPS at the pth and the qth bus may be derived as follows [15,20]:

$$P_{ps} = -G_{pq}V_p^2\tan^2\phi - V_pV_q\tan\phi[G_{pq}\sin(\delta_p - \delta_q) - B_{pq}\cos(\delta_p - \delta_q)] \quad (11)$$

$$Q_{ps} = B_{pq}V_p^2\tan^2\phi + V_pV_q\tan\phi[G_{pq}\cos(\delta_p - \delta_q) + B_{pq}\sin(\delta_p - \delta_q)] \quad (12)$$

$$P_{qs} = -V_pV_q\tan\phi\left[G_{pq}\sin(\delta_p - \delta_q) + B_{pq}\cos(\delta_p - \delta_q)\right] \quad (13)$$

$$Q_{qs} = -V_pV_q\tan\phi\left[G_{pq}\cos(\delta_p - \delta_q) - B_{pq}\sin(\delta_p - \delta_q)\right] \quad (14)$$

P_{ps}, Q_{ps} are the injected real and reactive powers at bus p due to TCPS, respectively and P_{qs}, Q_{qs} are the injected real and reactive powers at bus q due to TCPS, respectively.

Mathematical problem formulation

The objective of OPF is to minimize an objective function while satisfying all the equality and inequality constraints. The optimization problem of the present work, i.e. OPF problem incorporated with two FACTS devices like TCSC and TCPS deals with four different objective function while satisfying all equality and inequality constraints as well as the physical operating limits of the used FACTS devices.

The general formulation of this type of problem may be expressed as a constrained optimization problem as follows

$$Min\ \boldsymbol{of}(\boldsymbol{u}, \boldsymbol{v}) \quad (15)$$

$$\text{Subject to}: \begin{Bmatrix} g(\boldsymbol{u}, \boldsymbol{v}) = 0 \\ h(\boldsymbol{u}, \boldsymbol{v}) \leqslant 0 \end{Bmatrix} \quad (16)$$

where $\boldsymbol{of}$ is the objective function to be minimized; $g(\boldsymbol{u}, \boldsymbol{v})$ is the set of equality constraints; $h(\boldsymbol{u}, \boldsymbol{v})$ is the set of inequality constraints; $\boldsymbol{u}$ is the vector of dependent variables consisting of generator active power output at slack bus P_{G1}, load voltages $(V_{L1}, \ldots, V_{LN_{PQ}})$, generators' reactive powers $(Q_{G1}, \ldots, Q_{GN_{PV}})$, transmission line loadings $(S_{L1}, \ldots, S_{LN_L})$ and $\boldsymbol{v}$ is the vector of independent variables consisting of generators' active powers except slack bus $(P_{G2}, \ldots, P_{GN_{PV}})$, generators' voltages $(V_{G1}, \ldots, V_{GN_{PV}})$, transformers' tap settings $(T_1, \ldots, T_{N_T})$ and reactive power injections $(Q_{C1}, \ldots, Q_{CN_C})$. Therefore, $\boldsymbol{u}$ and $\boldsymbol{v}$ may be expressed as [15,20]:

$$\boldsymbol{u} = \lfloor P_{G1}, V_{L1}, \ldots, V_{LN_{PQ}}, Q_{G1}, \ldots, Q_{GN_{PV}}, S_{L1}, \ldots, S_{LN_L} \rfloor \quad (17)$$

$$\boldsymbol{v} = \lfloor P_{G2}, \ldots, P_{GN_{PV}}, V_{G1}, \ldots, V_{GN_{PV}}, T_1, \ldots, T_{N_T}, Q_{C1}, \ldots, Q_{CN_C} \rfloor \quad (18)$$

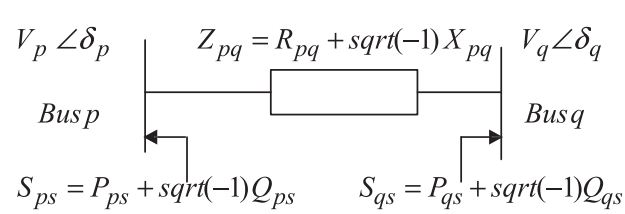

Fig. 3. Power injected model of TCPS connected between pth and qth bus.

where N_{PV} is the number of generator buses, N_{PQ} is the number of load buses, N_L is the number of transmission lines, N_T is the number of tap setting transformer branches and N_C is the number of capacitor banks.

Constraints

Here, g is the set of equality constraints representing the load flow equations as follows [15,20]:

$$\left.\begin{aligned}\sum_{p=1}^{N_B}(P_{Gp}-P_{Lp})+\sum_{p=1}^{N_{TCPS}}P_{pk}&=\sum_{p=1}^{N_B}\sum_{q=1}^{N_B}|V_p||V_q||Y_{pq}|\cos(\theta_{pq}+\delta_p-\delta_q)\\ \sum_{p=1}^{N_B}(Q_{Gp}-Q_{Lp})+\sum_{p=1}^{N_{TCPS}}Q_{pk}&=-\sum_{p=1}^{N_B}\sum_{q=1}^{N_B}|V_p||V_q||Y_{pq}|\sin(\theta_{pq}+\delta_p-\delta_q)\end{aligned}\right\} \tag{19}$$

where P_{Gp}, Q_{Gp} are the real and reactive power generations of the pth bus, respectively; P_{Lp}, Q_{Lp} are the real and reactive power demands of the pth bus, respectively; P_{pk}, Q_{pk} are the injected real and reactive powers of TCPS at the pth bus, respectively; Y_{pq} is the total admittance of the transmission line connected between the pth and the qth bus; θ_{pq} is the corresponding admittance angle of the transmission line connected between pth and qth bus; N_B is the total number of buses and N_{TCPS} is the number of TCPS devices connected in the power network.

In (16), h is the set of system operating limits that includes the constraints as mentioned below:

Generator real and reactive power outputs

Generator real and reactive power outputs of the pth unit should lie between their minimum and maximum limits as follows [15,20]:

$$P_{Gp}^{min} \leqslant P_{Gp} \leqslant P_{Gp}^{max}, \quad p=1,2,\ldots,N_{PV} \tag{20}$$

$$Q_{Gp}^{min} \leqslant Q_{Gp} \leqslant Q_{Gp}^{max}, \quad p=1,2,\ldots,N_{PV} \tag{21}$$

where P_{Gp}^{min} and P_{Gp}^{max} are the minimum and maximum limits of real power of the pth generating unit, respectively and Q_{Gp}^{min} and Q_{Gp}^{max} are the minimum and maximum limits of reactive power of the pth generating unit, respectively.

Voltage magnitudes at each bus in the network

Load bus voltage should lie between its respective minimum and maximum limits and may be represented as [15,20]:

$$V_{Lp}^{min} \leqslant V_{Lp} \leqslant V_{Lp}^{max}, \quad p=1,2,\ldots,N_{PQ} \tag{22}$$

where V_{Lp}^{min} and V_{Lp}^{max} are the minimum and maximum load voltage of the pth load bus, respectively.

Transformer tap settings

Transformer tap settings are bounded between minimum and maximum limits as given below [15,20]:

$$T_p^{min} \leqslant T_p \leqslant T_p^{max}, \quad p=1,2,\ldots,N_T \tag{23}$$

where T_p^{min} and T_p^{max} are the minimum and maximum tap setting limits of the pth transformer, respectively.

Shunt VAR compensator constraints

Shunt compensation of the pth compensator are restricted by their minimum and maximum limits as given by [15,20]:

$$Q_{Cp}^{min} \leqslant Q_{Cp} \leqslant Q_{Cp}^{max}, \quad p=1,2,\ldots,N_C \tag{24}$$

where Q_{Cp}^{min} and Q_{Cp}^{max} are the minimum and maximum VAR injection limits of the pth shunt capacitor, respectively.

Transmission lines loading

Line flow through each transmission line must be within its capacity limits and these may be represented as [15,20]:

$$S_{Lp} \leqslant S_{Lp}^{max}, \quad p=1,2,\ldots,N_L \tag{25}$$

where S_{Lp} and S_{Lp}^{max} are the apparent power flow of the pth branch and maximum apparent power flow limit of pth branch, respectively.

TCSC reactance constraints

TCSC reactances should lie within their respective minimum and maximum limits represented as [15,20]:

$$X_{Tp}^{min} \leqslant X_{Tp} \leqslant X_{Tp}^{max}, \quad p=1,2,\ldots,N_{TCSC} \tag{26}$$

where X_{Tp}^{min} and X_{Tp}^{max} are the minimum and maximum reactance of the pth TCSC, respectively, and N_{TCSC} is the number of TCSC devices installed in the test power system.

TCPS phase shift constraints

TCPS phase shifts should lie within their respective minimum and maximum boundaries given by [15,20]:

$$\phi_{Tp}^{min} \leqslant \phi_{Tp} \leqslant \phi_{Tp}^{max}, \quad p=1,2,\ldots,N_{TCPS} \tag{27}$$

where ϕ_{Tp}^{min} and ϕ_{Tp}^{max} are minimum and maximum phase shift angle of the pth TCPS, respectively, and N_{TCPS} is the number of TCPS devices installed in the test power system.

Objective function

In this article, four different objective functions are considered separately, to determine the superiority and effectiveness of the proposed algorithm. These objective functions are presented in the next four sub-sections.

Minimization of fuel cost

In this simulation study, the total generation cost is considered as an objective function. The fuel costs considered in this article are, mainly, of two types *viz.* (a) fuel cost with quadratic cost function and (b) fuel cost with valve point loading effect.

Fuel cost with quadratic cost function. The total fuel cost of generating units having quadratic cost function without valve point effect is given by [37,38]:

$$F_C=\sum_{p=1}^{N_{PV}}(a_p+b_pP_{G_p}+c_pP_{Gp}^2) \tag{28}$$

where a_p, b_p and c_p are the fuel cost coefficients of the pth generator.

Fuel cost with valve point loading effect. In practical generator, multiple valve steam turbines may be incorporated to achieve more accurate and flexible operation and, therefore, the valve point effect should also be considered to represent accurate cost function. The total cost of generating units with valve point loading effect is presented as [14,15]:

$$F_C=\sum_{p=1}^{N_{PV}}a_p+b_pP_{Gp}+c_pP_{Gp}^2+\left|d_p\sin(e_p(P_{Gp}^{min}-P_{Gp}))\right| \tag{29}$$

where d_p and e_p are the fuel cost coefficients with valve point loading effect of the pth generator.

Minimization of transmission loss

Mathematical formulation of this type of objective function is given by [14,15]:

$$Min\ P_{Loss} \tag{30}$$

It can also be, mathematically, formulated as:

$$P_{Loss} = \sum_{k=1}^{N_L} G_k[V_p^2 + V_q^2 - 2|V_p||V_q|\cos(\delta_p - \delta_q)] \tag{31}$$

where P_{Loss} is the total power loss and G_k is the conductance of the kth line connected between the pth and the qth buses.

Minimization of emission

Mathematical formulation of this type of problem can be written as:

$$Min\ E(P_g) \tag{32}$$

where $E(P_g)$ is the total emission.Thermal generating units emit atmospheric pollutants like nitrogen oxides (NO_x) and sulphur oxides (SO_x) which can be modelled separately. But for the sake of comparison, the total emission of these pollutants (which is the sum of a quadratic and an exponential function) may be expressed as [14,15]:

$$E(P_g) = \sum_{p=1}^{N_{PV}} \left(\alpha_p + \beta_p P_{Gp} + \gamma_p P_{Gp}^2 + \eta_p \exp(\lambda_p P_{Gp})\right) \tag{33}$$

where α_p, β_p, γ_p, η_p and λ_p are the emission coefficients of the pth generator.

Minimization of combined economic and environmental cost

The combined economic and environmental cost of OPF problem considers both cost and emission simultaneously. In this case, both economic and environmental OPF problem has been converted into a single objective optimization problem by introducing price penalty factor (PF) [37] and may be described as [15,20]:

$$Min\ OF(FU, E) \tag{34}$$

where $OF(FU, E)$ is the combined economic environmental cost and it may be, alternatively, formulated as [15,20]:

$$Min\ OF(FU, E) = Min\ \{FU + PF \times E\} \tag{35}$$

KHA

The krill herd algorithm [21] is based on the herding behaviour of krill swarms in response to specific biological and environmental processes. As KHA is a meta-heuristic one, two main characteristics may be noted here as, one is exploration or random search and other is exploitation or local search. Combination of these two plays a very important role to achieve highest performance in solving optimization problem.

In KHA, the objective function is, mainly, defined as the distance of food from each individual krill and the highest density of the herd. The time dependent position of each individual krill is determined by three main processes. These are [24]:

(a) movement induced by other krill individuals,
(b) foraging activity and
(c) random diffusion.

Regular KHA may be expressed by Lagrangian model in an n dimensional decision space as shown below [21]:

$$\frac{dx_i}{dt} = V_i^{new} + V_{F_i}^{new} + V_{D_i}^{new} \tag{36}$$

where V_i^{new} is the motion induced by other krill individuals, $V_{F_i}^{new}$ is the foraging motion and $V_{D_i}^{new}$ is the physical diffusion of the krill individuals.

Motion induced by other krill individuals

In this process, the krill individuals try to maintain a high density and the velocity of each individual is influenced by the movement of the others. The direction of motion induced (ψ_i) is, approximately, evaluated by the three effects namely (i) local effect, (ii) target effect and (iii) repulsive effect. For an individual krill i, this motion may be formulated as given below [29]:

$$V_i^{new} = \psi_i V_i^{\max} + \alpha V_i^{old} \tag{37}$$

$$\psi_i = \sum_{j=1}^{n_s} \left[\frac{z_i - z_j}{z_w - z_b} \times \frac{x_i - x_j}{|x_i - x_j| + rand(0,1)}\right] + 2\left[rand(0,1) + \frac{i}{i_{max}}\right] z_i^{best} X_i^{best} \tag{38}$$

where V_i^{max} is the maximum induced motion; α is the inertia weight of the motion induced in the range [0,1]; V_i^{old} is the previous induced motion of the ith krill individuals; z_w and z_b are the worst and best position among all krill individuals of the population, respectively; z_i and z_j are the fitness values of the ith and jth individuals; n_s is the number of krill individuals other than the particular krill; i and i_{max} are the number of current iteration and maximum number of iterations, respectively, and x represents the related positions.

For the determination of distance of individual krills and that of neighbours, a parameter named as sensing distance (D_s) is used. The sensing distance may be formulated as [31]:

$$D_s = \frac{1}{5N_i} \sum_{k=1}^{N_i} |x_i - x_k| \tag{39}$$

where N_i is the total number of the krill individual and x_k is the position of the kth krill. It is noted that if the distance between two individual krills has lesser values than the sensing distance then they are neighbours.

Foraging activity

Foraging activity is based upon two main factors. First is the present food location and second is the information about the previous food location. The foraging velocity may be expressed for ith krill individual as follows [21]:

$$V_{F_i}^{new} = 0.02\left[2\left(1 - \frac{i}{i_{max}}\right) z_i \frac{\sum_{k=1}^{n_s} \frac{x_k}{z_k}}{\sum_{k-1}^{n_s} \frac{1}{z_j}} + z_i^{best} X_i^{best}\right] + \alpha_F V_{F_i}^{old} \tag{40}$$

where α_F is the inertia weight of the foraging motion and $V_{F_i}^{new}$ and $V_{F_i}^{old}$ are the foraging motion of the ith krill, respectively.

Random diffusion

The random diffusion process of the krill individuals is, mainly, considered to enhance the population diversity. It may be expressed as follows [21]:

$$V_{D_i}^{new} = \xi V_D^{max} \tag{41}$$

where V_D^{max} is the maximum diffusion speed and ξ is the random directional vector lies between [−1,1].

Position update

In this process, the individual krill alters its current positions and moves to the better positions based on induction motion, foraging motion and random diffusion motion. According to the three above analysed motions, the updated position of the ith krill individual may be expressed as [22]:

$$x_i^{new'} = x_i^{new} + (V_i^{new} + V_{F_i}^{new} + V_{D_i}^{new})P_C\sum_{j=1}^{n_d}(u_j - l_j) \tag{42}$$

where n_d is the total number of variables; u_j and l_j are the upper and lower limits of the qth variables (j = 1, 2, . . . , n_d), respectively and P_C is the position constant number between [0,2].

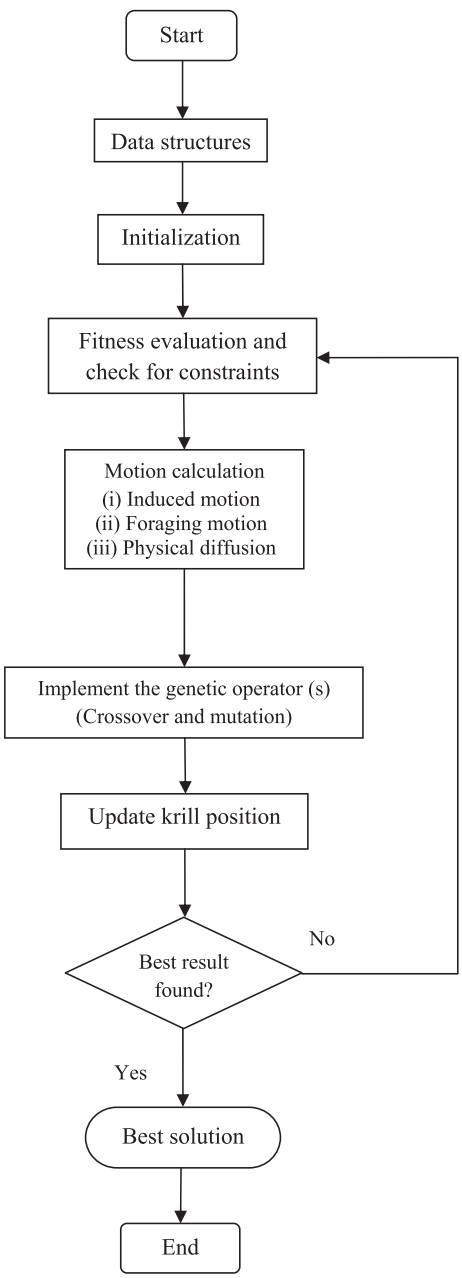

Fig. 4. Flowchart of KHA.

In order to improve the performance of the optimization problem and speed up the convergence property, the crossover and mutation process of DE algorithm is incorporated in KHA [21].

Crossover

Crossover process is, mainly, controlled by a parameter (termed as crossover probability (CR)). To update the position of own, each individual krill interacts with others. In this process, the jth component of the ith krill may be formulated as [31]:

$$x_{i,j} = \begin{cases} x_{k,j} & \text{if } rand \leqslant CR \\ x_{i,j} & \text{if } rand > CR \end{cases} \quad \text{where} \begin{cases} k = 1, 2, \ldots, N_p \\ k \neq p \end{cases} \tag{43}$$

$$CR = 0.2z_i^{best} \tag{44}$$

Mutation

Mutation process is, mainly, controlled by a parameter (named as mutation probability (MR)). This process may be formulated as [31]:

$$x_{i,j} = x_{best,j} + \gamma(x_{m,j} - x_{n,j}) \tag{45}$$

where $x_{best,j}$ is the global best vector; $x_{m,j}$ and $x_{n,j}$ are two randomly selected vectors and γ is a scalar number between 0 and 1.

The modified value of $x_{i,j}$ is formulated as follows [31]:

$$x_{i,j}^{\text{mod}} = \begin{cases} x_{i,j}^{new} & \text{if } rand \leqslant MR \\ x_{i,j} & \text{if } rand > MR \end{cases} \tag{46}$$

Computational procedure

The flowchart of the KHA is shown in Fig. 4. The computational procedure of this algorithm is illustrated in Algorithm 1.

Algorithm 1: Computational procedure for KHA

Step 1 *Initialization.* Set the parameters like; population size (N_p), maximum number of fitness function evaluation ($NFFE_{max}$), maximum induced speed (V_i^{max}), foraging speed (V_F) and maximum diffusion speed ($V_{D_i}^{new}$).

Step 2 *Fitness evaluation.* Generate randomly the position set of each krill individual and evaluate the fitness function value for each krill individual

Step 3 ***while*** the termination criteria is not satisfied or $t < NFFE_{max}$ ***do***
Sort the population from best to worst.
Store the best krill in KEEP.
for $i = 1 : N_p$ (all population) ***do***
Calculate the following motions;
(a) induced motion
(b) foraging motion
(c) physical diffusion
Update the position of the krill individual in the search space.
Evaluate each individual krill according to its new position.
end for
Replace the KEEP with best value.
Sort the population from best to worst and find the current best.
$t = t + 1$;

Step 4 ***end while***

Step 5 Post-procession of the results.

OKHA

OBL

OBL is, basically, a machine intelligence strategy which was proposed by Tizhoosh in [32]. It considers the current individual and its opposite individual simultaneously in order to get a better approximation at the same time for a current candidate solution. It has been also proved that an opposite candidate solution has a greater opportunity to be closer to the global optimal solution than a random candidate solution [39]. So, the concept of OBL has been utilised to enhance population based algorithms in [34,40–42].

The general, OBL concept has been, successfully, applied in some areas of research work such as in reinforcement learning [43], window memorization for morphological algorithms [44], image processing using the opposite fuzzy sets [45,46] and also in some popular optimization techniques like ant colony optimization [47–49], GA [50], artificial neural networks with opposite transfer function and back propagation [51,52], DE [41,42], PSO with Cauchy mutation [34,53], gravitational search algorithm [38], harmonic search algorithm [54], and BBO [55,56].

In proposing this technique, two definitions, namely, opposite point and opposite number and two steps, namely, opposition based population initialization and opposition based generation jumping are clearly defined below:

Opposite number

Let $m \in [x, y]$ be a real number. The opposite number of m (m^*) is defined by:

$$M^* = x + y - m \tag{47}$$

Opposite point

Let, $M = (m_1, m_2, \ldots, m_d)$ be a point in d-dimensional search space, where $m_r \in [x_r, y_r]$ and $d = \{1, 2, \ldots, d, \ldots, n\}$. The opposite point is defined by

$$m_r^* = x_r + y_r - m_r \tag{48}$$

Opposition based population initialization

By utilising opposite points, a suitable starting candidate solution may be obtained even when there is not a priori knowledge about the solution. The main steps of the proposed approach are listed as follows:

Step 1: Initialize the population set $M(N_r)$ in a random manner.
Step 2: Calculate opposite population by:

$$OM_{a,b} = x_b + y_b - M_{a,b} \tag{49}$$

where $a = 1, 2, \ldots, N_p$, $b = 1, 2, \ldots, n$ and $M_{a,b}$ and $OM_{a,b}$ denote the bth variable of the ath vector of the population and opposite population, respectively.

Step 3: Select the fittest N_p individuals from $\{M \cup OM\}$ as initial population.

The computational procedure of the above method is depicted in Algorithm 2.

Algorithm 2: Computational procedure for opposition based population initialization

Step 1 ***for*** $a = 1: N_p$
  for $b = 1: N$
    $OM_{a,b} = x_b + y_b - M_{a,b}$
  end for
end for
Step 2 Select N_p fittest individuals from set of $\{M \cup OM\}$.

Opposition based generation jumping

If we apply similar approach to the current population, the whole evolutionary process can be forced to jump to a new solution candidate which is more suitable than the current one. Based on a jumping rate (J_R), after following the induction, foraging action and random diffusion processes of KHA, the new population is generated and opposite population is calculated. From this comparison, the fittest N_p individuals are selected. In each generation, search space is reduced to calculate the opposite points, i.e.

$$OM_{a,b} = Min_b^{gn} + Max_b^{gn} - M_{a,b} \tag{50}$$
$$a = 1, 2, \ldots, N_p \text{ and } b = 1, 2, \ldots, n$$

where $\lfloor Min_b^{gn}, Max_b^{gn} \rfloor$ is the current interval in the population which is becoming increasingly smaller than the corresponding initial range $[x_b, y_b]$.

The computational procedure of this algorithm is illustrated in Algorithm 3.

Algorithm 3: Computational procedure for opposition based generation jumping

Step 1 ***if*** $(rand_1 < J_R)$**%** $rand_1 \in [0, 1]$, J_R: Jumping rate
  for $a = 1: N_p$
    for $b = 1: N$
      $OM_{a,b} = Min_b^{gn} + Max_b^{gn} - M_{a,b}$
        % Min_b^{gn}: minimum value of the bth variable in the current generation (gn)
        % Max_b^{gn}: maximum value of the bth variable in the current generation (gn)
      Select N_p fittest individuals from set of $\{M \cup OM\}$.
    end for
  end for
end if
Step 2 Select N_p fittest individuals from set of $\{M \cup OM\}$.

Flowchart of OKHA

The flowchart of the proposed OKHA is shown in Fig. 5.

Implementation of OKHA for OPF problem with FACTS

The main steps of the proposed OKHA approach, as applied to OPF problem with FACTS devices are described in Algorithm 4.

Algorithm 4: OKHA for OPF problem with FACTS devices

Step 1	Read the parameters of power system (line data, bus data, fuel cost co-efficient, load flow parameters, etc.) as well as those of the proposed algorithm and specify the upper and lower limits of each individual parameter like (a) active power generation, (b) generator bus voltage, (c) load bus voltage, (d) reactive power generation, (e) tap changing transformers, (f) shunt compensating devices, (g) line flow through each transmission line and most importantly TCSC reactance and TCPS phase shift constraints. Afterward, initialised again. Now several initial set depending upon the population size are generated. A feasible solution set (control variables) represents the position of different krill individuals.
Step 2	For determining the feasible population set of OBL, all the parameters of power system and the proposed algorithm have to be initialized within its upper and lower limit (refer Algorithm 1). Then, Newton Raphson based load flow [36,57] method is run to check if these constraints are within the limits or not. If anyone of them violates the limits then corresponding set is discarded and reinitialised. Thus, the feasible solution set is obtained.
Step 3	Select the fittest individuals.
Step 4	Sort them from best to worst.
Step 5	Choose N_p elite solutions based on the fitness value.
Step 6	The position of krill individuals of non elite population set is modified. Further, application of crossover and mutation operation again modifies the position.
Step 7	Run Newton Raphson based load flow [36,57] to determine the dependent variables of OPF problem with FACTS devices and evaluate the fitness value of population set.
Step 8	Based on (J_R), the new opposite population and corresponding fitness values are calculated (refer Algorithm 2). Newton Raphson [36,57] based load flow is run to check if the constraints are within the limits or not. If any one of them does not satisfy the inequality constraints, then that particular set have to be discarded and
Step 9	Check for the constraints of the problem.
Step 10	Go to **Step 6** until a stopping criterion is satisfied.

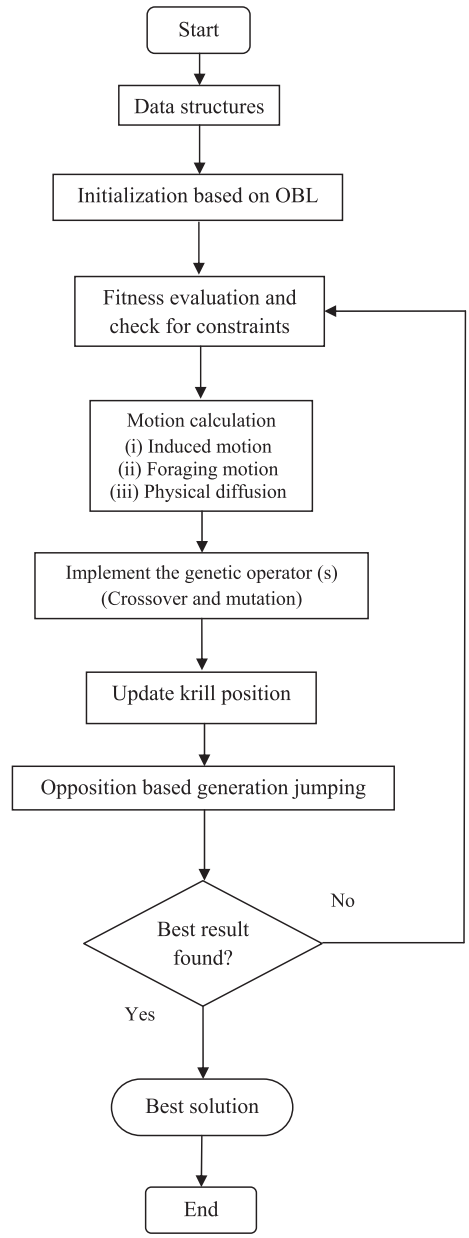

Fig. 5. Flowchart of OKHA.

Simulation results and discussion

In order to demonstrate the applicability and validity of the proposed OKHA algorithm for OPF problems having TCSC and TCPS devices located at fixed locations, two different test systems *viz.* modified IEEE-30 bus and IEEE-57 bus power systems are considered. All the simulations are carried out using MATLAB 2008a computing environment on a 2.63 GHz Pentium IV personal computer with 3 GB RAM. For establishing the superiority of the proposed OKHA, thirty independent test trial runs are performed for all the test cases and simulation results along with comparative discussion are reported in this part. The value of $NFFE_{max}$ is set as 500 for all the simulated test cases. To indicate the optimization capability of the proposed OKHA, the results of interest are **bold faced** in the respective tables.

Test system 1: Modified IEEE-30 bus test power system

The modified IEEE-30 bus test system consists of six generating units (at buses 1, 2, 5, 8, 11, 13) and twenty-four load buses interconnected with forty-one transmission lines of which four branches (6–9, 6–10, 4–12 and 28–27) equipped with tap changing transformer and nine branches having shunt VAR compensators (at buses 10, 12, 15, 17, 20, 21, 23, 24 and 29) is considered as test system 1. Bus 1 is selected as the slack bus. The total system demand is 2.834 p.u. at 100 MVA base. The load bus voltages have been constrained within the ranges of 0.95–1.05 p.u. In this test system, two TCSCs are incorporated in the branches like {3,4} and {19,20} and two TCPSs are installed in branches like {5,7} and {10,22}, respectively, in line with [15,20].

Table 1
Best control variable settings for fuel cost (without valve point effect) minimization objective of modified IEEE-30 bus test power system offered by different algorithms.

Control variables	TS/SA [17]	DE [14]	ALC-PSO [20]	KHA (studied)	OKHA (proposed)
P_{G1} (MW)	192.46	180.26	185.24	194.80	194.65
P_{G2} (MW)	48.38	49.32	46.33	49.65	49.76
P_{G5} (MW)	19.54	20.82	20.88	15.00	15.00
P_{G8} (MW)	11.60	17.61	15.64	10.00	10.00
P_{G11} (MW)	10.00	11.05	11.12	10.00	10.00
P_{G13} (MW)	12.00	12.69	12.58	12.00	12.00
Total P_G (MW)	294.00	291.75	291.79	291.45	291.41
Xc_{3-4} (p.u.)	0.0200	0.0190	0.0192	0.0148	0.0157
Xc_{19-20} (p.u.)	0.0200	0.0243	0.0241	0.0201	0.0214
ϕ_{5-7} (°)	1.9137	−0.5558	−0.5556	−0.5510	−0.5504
ϕ_{10-22} (°)	0.8251	−0.0286	−0.0287	−0.0251	−0.0251
Cost ($/h)	803.84	797.29	796.93	796.408	**796.289**
Emission (ton/h)	NR*	0.3756	0.390207	0.424966	0.424469
P_{Loss} (MW)	10.60	8.35	8.39	8.05	8.01
CPU time (s)	265.8	487.3	479.2	470.28	458.1

NR* means not reported in the referred literature.

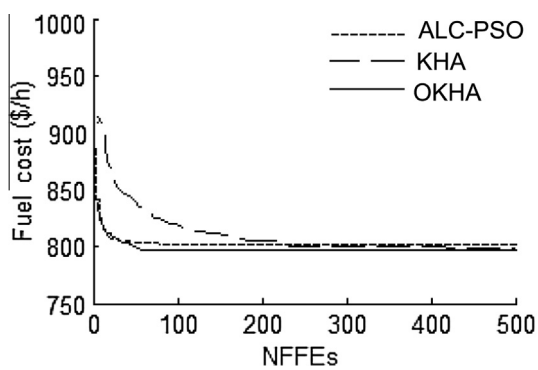

Fig. 6. Comparative convergence profile of fuel cost for fuel cost with quadratic fuel cost minimization objective of modified IEEE-30 bus test power system.

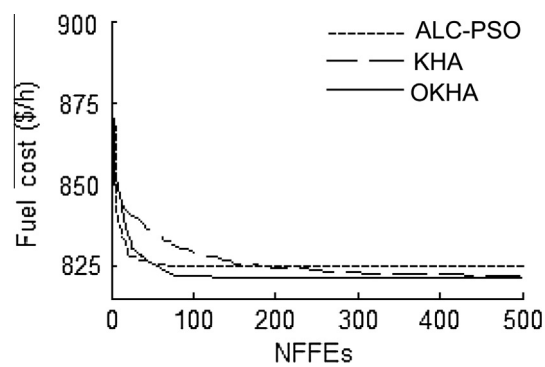

Fig. 7. Comparative convergence profile of fuel cost for fuel cost with valve point effect minimization objective of modified IEEE-30 bus test power system.

Case study 1: Minimization of fuel cost

(i) Without considering valve point effect: Both KHA and OKHA based results of OPF problem with FACTS devices for fuel cost minimization objective of this test system is presented in Table 1. These results are compared with TS/SA [17], DE [14] and ALC-PSO [20] and these results are also featured in the same table. It may be observed from this table that the minimum fuel cost as obtained from the proposed OKHA, is **796.289 $/h** which is less by **0.08%** compared to the previously reported best results of 796.93 $/h [20]. The fuel cost for KHA is found to be 796.408 $/h. The comparative convergence profile of fuel cost ($/h) for this power system, as yielded by ALC-PSO, studied KHA and the proposed OKHA, is presented in Fig. 6. From this figure it is observed that the fuel cost function value converges smoothly at lesser iteration cycles for OKHA than the other two.

(ii) With valve point effect: Table 2 represents the best control variables for the solution of OPF problem with FACTS devices for fuel cost minimization objective considering valve point loading effect for this test system. The results obtained from both KHA and OKHA are compared with other optimization

Table 2
Best control variable settings for fuel cost minimization objective (with valve point effect) of modified IEEE-30 bus test power system offered by different algorithms.

Control variables	RCGA [14]	DE [14]	ALC-PSO [20]	KHA (studied)	OKHA (proposed)
P_{G1} (MW)	198.81	199.13	199.85	200.000	200.000
P_{G2} (MW)	38.96	38.32	38.20	45.106	45.000
P_{G5} (MW)	19.16	20.17	20.16	15.012	15.100
P_{G8} (MW)	10.64	11.43	11.15	10.000	10.000
P_{G11} (MW)	13.56	10.43	10.13	10.000	10.000
P_{G13} (MW)	12.03	12.66	12.66	12.000	12.000
Total P_G (MW)	293.16	292.14	292.15	292.118	292.10
Xc_{3-4} (p.u.)	0.0185	0.0123	0.0122	0.0123	0.0119
Xc_{19-20} (p.u.)	0.0247	0.0250	0.0251	0.0251	0.0248
ϕ_{5-7} (°)	−0.5713	−0.1891	−0.1819	−0.1821	−0.1801
ϕ_{10-22} (°)	−0.0281	0.2177	0.2148	0.2145	0.2114
Cost ($/h)	831.03	826.54	825.89	824.18	**824.09**
Emission (ton/h)	0.4366	0.4383	0.441245	0.443735	0.443705
P_{Loss} (MW)	9.76	8.74	8.75	8.718	8.70
CPU time (s)	714.8	505.6	503.12	499.89	490.12

Table 3
Best control variable settings for active power transmission loss minimization objective of modified IEEE-30 bus test power system offered by different algorithms.

Control variables	RCGA [14]	DE [14]	ALC-PSO [20]	KHA (studied)	OKHA (proposed)
P_{G1} (MW)	77.58	74.59	74.69	74.526	74.521
P_{G2} (MW)	69.58	67.30	67.30	67.601	67.590
P_{G5} (MW)	49.98	50.00	50.00	50.000	50.000
P_{G8} (MW)	34.96	34.85	34.66	34.431	34.322
P_{G11} (MW)	23.69	27.04	27.26	27.111	27.244
P_{G13} (MW)	30.43	32.36	32.22	32.454	32.431
Total P_G (MW)	286.22	286.14	286.13	286.123	286.108
Xc_{3-4} (p.u.)	0.0193	0.0084	0.0081	0.0081	0.0071
Xc_{19-20} (p.u.)	0.0239	0.0045	0.0044	0.0041	0.0034
ϕ_{5-7} (°)	−0.5347	−0.5329	−0.5327	−0.5311	−0.5314
ϕ_{10-22} (°)	−0.0292	−0.4526	−0.4527	−0.4514	−0.4517
Cost ($/h)	985.21	992.30	992.18	992.14	992.43
Emission (ton/h)	0.2144	0.2109	0.210904	0.210920	0.210890
P_{Loss} (MW)	2.82	2.74	2.73	2.723	**2.708**
CPU time (s)	711.7	497.4	490.1	482.15	468.41

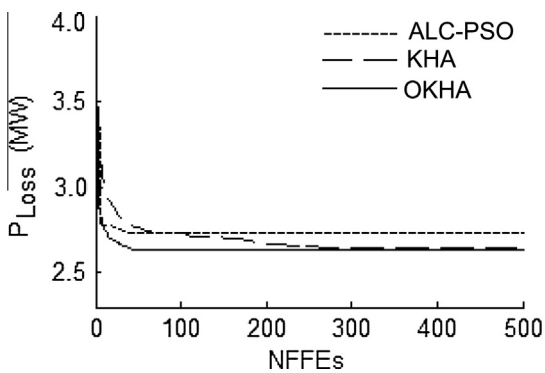

Fig. 8. Comparative convergence profile of P_{Loss} for P_{Loss} minimization objective of modified IEEE-30 bus test power system.

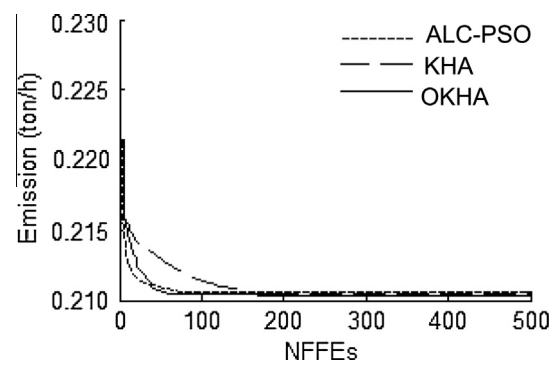

Fig. 9. Comparative convergence profile of emission for emission minimization objective of modified IEEE-30 bus test power system.

techniques such as RCGA [14], DE [14] and ALC-PSO [20] including the basic KHA one. This table shows that a fuel cost reduction of **0.2179%** is accomplished from the previous best of 825.89 $/h as reported by using ALC-PSO in [20] to **824.09 $/h.** Fig. 7. shows the comparative ALC-PSO, studied KHA and the proposed OKHA based convergence characteristics of fuel cost for fuel cost minimization objective considering valve point loading effect for this test system and the nature of the characteristic yielded by the proposed OKHA is found to be promising one.

Case study 2: Minimization of transmission active loss

Considering minimization of transmission active loss as one of the objective function for this modified IEEE-30 bus power system, obtained optimal values of the control variables from both KHA and the proposed OKHA techniques are reported in Table 3 along with the previously reported values yielded by RCGA [14], DE [14] and ALC-PSO [20]. The minimum real power loss, as obtained by using OKHA, is found to be **2.708 MW** which is **0.8058%** less than previously published best result offered by ALC-PSO [20]. This value of transmission active power loss is even found to be less than KHA based one. Promising convergence profile of

Table 4
Best control variable settings for emission minimization objective of modified IEEE-30 bus test power system offered by different algorithms.

Control variables	RCGA [14]	DE [14]	ALC-PSO [20]	KHA (studied)	OKHA (proposed)
P_{G1} (MW)	63.98	63.50	64.52	65.004	64.996
P_{G2} (MW)	67.75	67.92	66.90	66.371	66.375
P_{G5} (MW)	50.00	50.00	50.00	50.000	50.000
P_{G8} (MW)	35.00	35.00	35.00	35.000	35.000
P_{G11} (MW)	29.96	30.00	30.00	30.000	30.000
P_{G13} (MW)	40.00	40.00	40.00	40.000	40.000
Total P_G (MW)	286.69	286.42	286.42	286.375	286.371
Xc_{3-4} (p.u.)	0.0192	0.0187	0.0185	0.0180	0.0181
Xc_{19-20} (p.u.)	0.0246	0.0251	0.0249	0.0245	0.0234
ϕ_{5-7} (°)	−0.5518	−0.5478	−0.5462	−0.5141	−0.5414
ϕ_{10-22} (°)	−0.0288	0.0293	0.0291	0.0245	0.0245
Cost ($/h)	1015.80	1015.10	1014.24	1013.61	1013.61
Emission (ton/h)	0.2049	0.2048	0.204758	0.204755	**0.204754**
P_{Loss} (MW)	3.29	3.02	3.020	2.975	2.971
CPU time (s)	707.6	511.3	506.1	500.14	490.12

Table 5
Best control variable settings for combined fuel cost and emission minimization objective of modified IEEE-30 bus test power system offered by different algorithms.

Control variable	DE [14]	ALC-PSO [20]	KHA (studied)	OKHA (proposed)
P_{G1} (MW)	107.98	115.23	120.526	120.429
P_{G2} (MW)	58.57	56.57	53.278	53.371
P_{G5} (MW)	32.38	31.88	31.217	31.211
P_{G8} (MW)	27.61	27.54	27.240	27.237
P_{G11} (MW)	29.51	23.89	22.858	22.865
P_{G13} (MW)	33.27	34.22	34.212	34.208
Total P_G (MW)	289.32	289.33	289.331	289.321
Xc_{3-4} (p.u.)	0.0024	0.0021	0.0021	0.0019
Xc_{19-20} (p.u.)	0.0170	0.0168	0.0157	0.0156
ϕ_{5-7} (°)	0.6131	0.6128	0.5012	0.6117
ϕ_{10-22} (°)	−0.0745	−0.0743	−0.0732	−0.0712
OF	1238.099	1234.445	1232.942	**1232.895**
Cost ($/h)	922.36	907.17	897.41	897.51
Emission (ton/h)	0.2364	0.24302	0.249151	0.249045
P_{Loss} (MW)	5.92	5.93	5.931	5.921
CPU time (s)	521.9	515.1	508.14	498.12

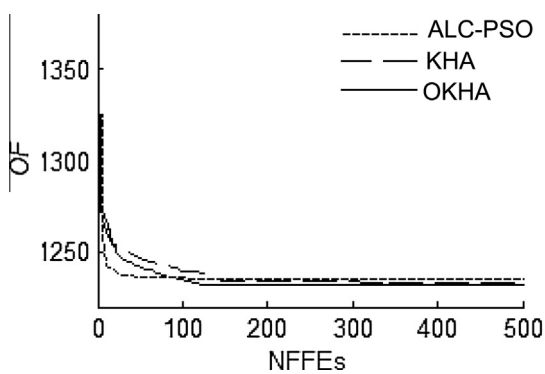

Fig. 10. Comparative convergence profile of *OF* for combined economic and environmental cost minimization objective of modified IEEE-30 bus test power system.

P_{Loss} (MW), as yielded by the proposed OKHA, is shown in Fig. 8. In the same figure, ALC-PSO and the studied KHA based convergence profiles of P_{Loss} (MW) are also included for the sake of comparison.

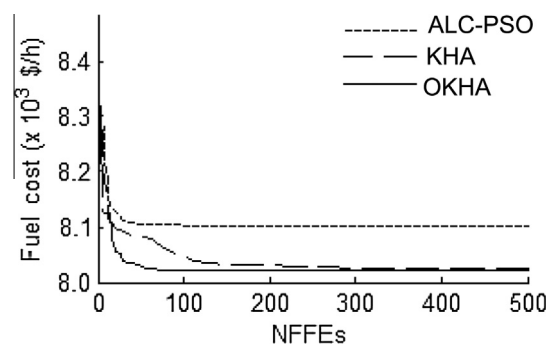

Fig. 11. Comparative convergence profile of fuel cost for fuel cost minimization objective of standard IEEE-57 bus test power system.

Case study 3: Minimization of emission

The best control variable settings for emission minimization of this test system, as yielded by both KHA and the proposed OKHA, are tabulated in Table 4. In this table, obtained KHA and OKHA based results are compared with other optimization techniques

Table 6
Best control variable settings for fuel cost minimization objective of IEEE-57 bus test power system offered by different algorithms.

Control variables	RCGA [14]	DE [14]	ALC-PSO [20]	KHA (studied)	OKHA (proposed)
P_{G1} (MW)	517.45	520.09	514.26	516.493	510.672
P_{G2} (MW)	0	0	0.00	0.000	6.321
P_{G3} (MW)	94.81	103.74	123.53	129.603	130.256
P_{G6} (MW)	0	0	0.00	0.000	0.000
P_{G8} (MW)	181.75	175.63	159.67	155.214	155.792
P_{G9} (MW)	0	0	0.00	0.000	0.000
P_{G12} (MW)	489.77	485.23	486.89	482.261	482.650
Total P_G (MW)	1283.78	1284.69	1284.35	1283.571	1285.691
Xc_{18-19} (p.u.)	0.0572	0.0604	0.0519	0.0413	0.0402
Xc_{31-32} (p.u.)	0.0832	0.0199	0.0233	0.0197	0.0224
Xc_{34-32} (p.u.)	0.0203	0.0015	0.0104	0.0014	0.0136
Xc_{40-56} (p.u.)	0.0480	0.0932	0.0439	0.0729	0.0771
Xc_{39-57} (p.u.)	0.0624	0.0466	0.0555	0.0457	0.0431
ϕ_{4-5} (°)	−0.7678	−0.6131	−0.8170	−0.6127	−0.5647
ϕ_{5-6} (°)	−0.7620	−0.6188	−0.6489	−0.6107	−0.5452
ϕ_{26-27} (°)	−0.3438	−0.4698	−0.5478	−0.4617	−0.5525
ϕ_{41-43} (°)	−0.3953	0.5099	0.4100	0.5067	0.1254
ϕ_{53-54} (°)	−0.4011	−0.1146	−0.2455	−0.1104	−0.1567
Cost ($/h)	8413.43	8309.27	8103.18	8030.28	**8029.64**
Emission (ton/h)	2.4331	2.4333	2.397822	2.398339	2.361343
P_{Loss} (MW)	32.98	33.89	33.55	32.771	34.891
CPU time (s)	874.9	689.9	680.12	650.9	637.25

Table 7
Best control variable settings for active power transmission loss minimization objective of IEEE-57 bus test power system offered by different algorithms.

Control variables	RCGA [14]	DE [14]	ALC-PSO [20]	KHA (studied)	OKHA (proposed)
P_{G1} (MW)	303.24	318.58	311.340	310.677	310.662
P_{G2} (MW)	0	0	0.000	0.000	0.000
P_{G3} (MW)	63.19	45.90	60.613	61.351	61.349
P_{G6} (MW)	0	0	0.000	0.000	0.000
P_{G8} (MW)	400.75	407.65	400.060	400.254	400.263
P_{G9} (MW)	0	0	0.000	0.000	0.000
P_{G12} (MW)	500.00	495.03	495.140	494.867	494.872
Total P_G (MW)	1267.18	1267.16	1267.153	1267.149	1267.146
Xc_{18-19} (p.u.)	0.0593	0.0100	0.0451	0.0101	0.0214
Xc_{31-32} (p.u.)	0.0179	0.0004	0.0014	0.0003	0.0010
Xc_{34-32} (p.u.)	0.0189	0.0079	0.0124	0.0079	0.0017
Xc_{40-56} (p.u.)	0.0641	0.0819	0.0781	0.0804	0.0711
Xc_{39-57} (p.u.)	0.0055	0.0841	0.0664	0.0848	0.0245
ϕ_{4-5} (°)	−0.6532	−0.0745	−0.0245	−0.0755	−0.0772
ϕ_{5-6} (°)	−0.0917	−0.2807	−0.3458	−0.2827	−0.2447
ϕ_{26-27} (°)	−0.7620	−0.9798	−0.8745	−0.9777	−0.7964
ϕ_{41-43} (°)	0.6933	−0.9053	−0.8974	−0.9054	−0.9047
ϕ_{53-54} (°)	0.2406	0.9798	0.9947	0.9791	0.8467
Cost ($/h)	15423.88	15691.30	15348.11	15356.31	15356.77
Emission (ton/h)	1.906545	1.966905	1.917299	1.914837	1.914828
P_{Loss} (MW)	16.38	16.36	16.353	16.349	**16.346**
CPU time (s)	881.3	701.7	691.045	671.2	654.11

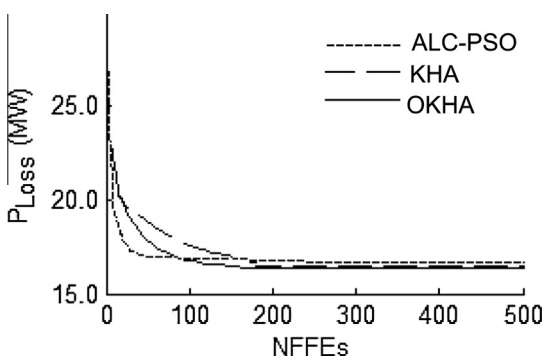

Fig. 12. Comparative convergence profile of P_{Loss} for P_{Loss} minimization objective of standard IEEE-57 bus test power system.

recently published in the literature like RCGA [14], DE [14] and ALC-PSO [20]. The value of emission yielded by OKHA (**0.204754 ton/h**) is improved by **0.0019535%** as compared to ALC-PSO based result (0.204758 ton/h) reported in [20]. It is also noted that this value of emission is even less than that offered by KHA. ALC-PSO, studied KHA and the proposed OKHA based comparative convergence profile of emission for this test system is given in Fig. 9 from which OKHA based one is found to be promising one.

Case study 4: Minimization of combined economic and environmental cost

Results of both KHA and OKHA based OPF solution for combined economic and environmental cost minimization objective for this test system are presented in Table 5 and those are compared to other optimization methods like DE [14] and ALC-PSO [20]. From this table, it may be noted that **0.1256%** reduction in combined economic and environmental cost takes place by using the proposed OKHA based algorithm may be noted as (**1232.895**) as compared to ALC-PSO may be noted as (1234.445) counterpart reported in [20]. The value of *OF* offered by KHA is found to be 1232.942 for this test system. Promising convergence profile of *OF*, as yielded by ALC-PSO, studied KHA and the proposed OKHA for this case study, may be observed from Fig. 10

Test system 2: Modified IEEE-57 bus test power system

The modified IEEE-57 bus test system consists of seven generating units at buses 1, 2, 3, 6, 8, 9, 12 interconnected with fifteen transformers under load tap settings is chosen as test system 2. Three reactive power sources are taken at buses 18, 25 and 53. All the bus data, line data and initial values of control variables are taken from [58,59]. The total system demand is 12.508 p.u. at 100 MVA base. In this work, TCSCs are incorporated in five lines like {18,19}, {31,32}, {34,32}, {40,56} and {39,57} and TCPSs are installed in five lines like {4,5}, {5,6}, {26,27}, {41,43} and {53,54} [15,20].

Case study 1: Minimization of fuel cost

The objective in this case is to minimize the total fuel cost. Table 6 depicts the comparative results of optimal settings of control variables for OKHA as well as KHA along with those offered by RCGA [14], DE [14] and ALC-PSO [20]. From this table, the fuel cost corresponding to OKHA may be noted as **8029.64 $/h** (i.e. **0.9075%** less compared to ALC-PSO [20]). The same yielded by ALC-PSO [20] may be noted as 8103.18 $/h. OKHA based results shows **0.008%** reduction in fuel cost as compared to KHA counterpart for this objective function. The comparative convergence characteristic offered by ALC-PSO, the studied KHA and the proposed OKHA is portrayed in Fig. 11 which presents that OKHA based objective function value converges faster as compared to ALC-PSO and KHA counterpart.

Case study 2: Minimization of transmission active loss

The results obtained for the transmission active loss minimization by the proposed OKHA are compared with other optimization methods like KHA, RCGA [14], DE [14] and ALC-PSO [20] (Table 7). It may be seen from this table that the obtained real power transmission loss from the proposed OKHA is **16.346 ton/h.** This proves loss reduction of **0.0428%** has taken place while adopting OKHA as compared to the previous algorithm like ALC-PSO [20]. The comparative ALC-PSO, studied KHA and proposed OKHA based convergence profile of P_{Loss} (MW), shown in Fig. 12, presents that OKHA converges faster as compared to the other two counterparts.

Table 8
Best control variable settings for emission minimization objective of IEEE-57 bus test power system offered by different algorithms.

Control variable	RCGA [14]	DE [14]	ALC-PSO [20]	KHA (studied)	OKHA (proposed)
P_{G1} (MW)	341.91	298.12	300.23	294.373	294.300
P_{G2} (MW)	0	0	0.00	0.000	0.000
P_{G3} (MW)	91.90	83.24	91.43	92.421	92.480
P_{G6} (MW)	0	0	0.00	0.000	0.000
P_{G8} (MW)	419.25	413.63	406.26	411.000	411.000
P_{G9} (MW)	0	0	0.00	0.000	0.000
P_{G12} (MW)	418.45	474.14	472.08	472.102	472.091
Total P_G (MW)	1271.51	1269.13	1270.00	1269.896	1269.871
Xc_{18-19} (p.u.)	0.0830	0.0830	0.0741	0.0819	0.0847
Xc_{31-32} (p.u.)	0.0672	0.0672	0.0789	0.0667	0.0554
Xc_{34-32} (p.u.)	0.0009	0.0009	0.0008	0.0008	0.0006
Xc_{40-56} (p.u.)	0.0437	0.0437	0.0450	0.0445	0.0552
Xc_{39-57} (p.u.)	0.0772	0.0772	0.0669	0.0766	0.0688
ϕ_{4-5} (°)	−0.8995	−0.8995	−0.8745	0.8937	−0.8966
ϕ_{5-6} (°)	0.4297	0.4297	0.2564	0.4299	0.5467
ϕ_{26-27} (°)	−0.8079	−0.8079	−0.7914	−0.8047	−0.8137
ϕ_{41-43} (°)	−0.1375	−0.1375	−0.2456	−0.1365	−0.2561
ϕ_{53-54} (°)	−1.0313	−1.0313	−1.1140	−1.0324	−1.0447
Cost ($/h)	15856.14	15914.38	15577.34	15809.78	15809.82
Emission (ton/h)	1.889188	1.858705	1.838714	1.835159	**1.834913**
P_{Loss} (MW)	20.71	18.33	19.20	19.096	19.071
CPU time (s)	878.7	694.2	690.14	675.3	666.12

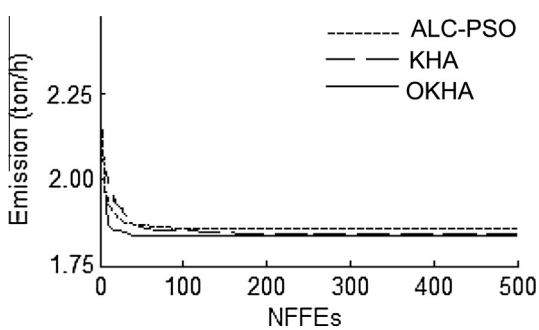

Fig. 13. Comparative convergence profile of emission for emission minimization objective of standard IEEE-57 bus test power system.

Case study 3: Minimization of emission

Table 8 compares the results obtained by both KHA and OKHA along with the other previously reported results offered by popular techniques like RCGA [14], DE [14] and ALC-PSO [20] considering emission minimization as an objective function for this test case. It may be noted from this table that an emission reduction of nearly **0.21 ton/h** is achieved while adopting OKHA (**1.834913 ton/h**) over the ALC-PSO (1.838714 ton/h) [20]. Comparative convergence profile, shown in Fig. 13, gives the effective convergence result for OKHA one.

Case study 4: Minimization of combined economic and environmental cost

The optimal values of control variables offered by both KHA and OKHA techniques for combined economic and environmental cost minimization objective function for this test power system are

Table 9
Best control variable settings for combined economic and environmental cost minimization objective of IEEE-57 bus test power system offered by different algorithms.

Control variable	DE [14]	ALC-PSO [20]	KHA (studied)	OKHA (proposed)
P_{G1} (MW)	475.68	480.93	480.969	480.830
P_{G2} (MW)	0.00	0.00	5.452	5.340
P_{G3} (MW)	80.64	82.14	92.376	92.270
P_{G6} (MW)	0.00	0.00	0.000	0.000
P_{G8} (MW)	276.03	270.42	259.004	258.980
P_{G9} (MW)	0.00	0.00	0.000	0.000
P_{G12} (MW)	447.20	446.04	442.218	442.140
Total P_G (MW)	1279.55	1279.53	1280.019	1279.560
Xc_{18-19} (p.u.)	0.0077	0.0084	0.0061	0.0067
Xc_{31-32} (p.u.)	0.0360	0.0267	0.0445	0.0447
Xc_{34-32} (p.u.)	0.0832	0.0789	0.8842	0.0771
Xc_{40-56} (p.u.)	0.0221	0.0159	0.0415	0.0358
Xc_{39-57} (p.u.)	0.0521	0.0489	0.0481	0.0480
ϕ_{4-5} (°)	0.8308	0.7795	0.8745	0.8921
ϕ_{5-6} (°)	−0.4526	−0.4697	−0.3441	−0.3447
ϕ_{26-27} (°)	−0.5500	−0.5459	−0.4495	−0.4940
ϕ_{41-43} (°)	−0.7277	−0.6987	−0.6582	−0.6543
ϕ_{53-54} (°)	0.8136	0.8135	−0.8314	0.8245
OF	13183.423	13032.568	12653.874	**12649.060**
Cost ($/h)	10408.49	10237.79	9898.54	9895.01
Emission (ton/h)	2.211635	2.227447	2.196009	2.194986
P_{Loss} (MW)	28.750	28.73	29.219	28.760
CPU time (s)	702.9	700.5	694.12	685.12

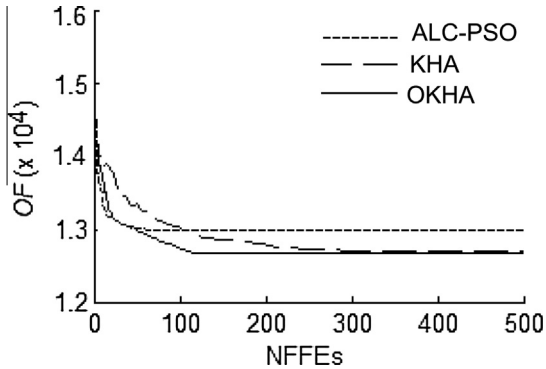

Fig. 14. Comparative convergence profile of *OF* for combined economic and environmental cost minimization objective of standard IEEE-57 bus test power system.

tabulated in Table 9. The other results like DE [14], ALC-PSO [20] are also shown in the same table for the sake of comparison. In this case, the obtained OKHA based obtained results indicate a reduction of **2.94%** in the value of *OF* as compared to ALC-PSO [20]. For this case study, the proposed OKHA offers the value of *OF* as **12649.06** while the same offered by ALC-PSO [20] is 13032.568. Fig. 14 portrays the comparative convergence characteristic of this objective function yielded by ALC-PSO, the studied KHA and the proposed OKHA and it is found that the proposed OKHA converges smoothly as compared to ALC-PSO and KHA counterparts.

Conclusion and scope of future work

In this article, a novel meta-heuristic algorithm like OKHA is proposed to solve the OPF problem of power system incorporated with FACTS devices. Four different objective functions *viz.* (i) minimization of fuel cost, (ii) minimization of power transmission active loss, (iii) emission reduction and (iv) combined economic and environmental cost minimization problem are formulated, individually, with due regard to the equality and the inequality constraints. To check the superiority of the proposed OKHA, it is tested on two different standard test power systems like modified IEEE-30 bus and modified IEEE-57 bus with TCSC and TCPS installed at fixed strategic locations. Simulation results offered by both OKHA and KHA are compared to other popular techniques recently reported in the recent state-of-the-art literature and it is demonstrated that better efficiency, robustness, stability and faster convergence rate are obtained while applying the proposed OKHA. So, it is explicitly shown in this article that this new algorithm may be very much promising and encouraging for the future research work. As some other scopes of future work, the following mentioned points may be noted down.

(a) The combined economic and environmental cost and transmission active power loss are considered in the present work separately. However, these two may be combined together to form a single cost function which may be minimized.
(b) Within the periphery of the present work, the cost of FACTS devices has not been considered. However, the same may be incorporated to re-formulate the problem.

References

[1] Momoh JA, EL-Hawary ME, Adapa R. A review of selected optimal power flow literature to 1993, part I: nonlinear and quadratic programming approach. IEEE Trans Power Syst 1999;14(1):96–104.
[2] Momoh JA, EL-Hawary ME, Adapa R. A review of selected optimal power flow literature to 1993, part II: Newton, linear programming and interior point methods. IEEE Trans Power Syst 1999;14(1):105–11.
[3] Monticelli A, Liu W. Adaptive movement penalty method for the Newton optimal power flow. IEEE Trans Power Syst 1992;7(1):334–42.
[4] Wei H, Sasaki H, Kubokawa J, et al. An interior point nonlinear programming for optimal power flow problems with a novel data structure. IEEE Trans Power Syst 1998;13(3):870–7.
[5] Devaraj D, Yegnanarayana B. Genetic-algorithm-based optimal power flow for security enhancement. Proc IEE Gener Transm Distrib 2005;152(6):899–905.
[6] Sood YR. Evolutionary programming based optimal power flow and its validation for deregulated power system analysis. Int J Electr Power Energy Syst 2007;29(1):65–75.
[7] Bhowmik AR, Chakraborty AK. Solution of optimal power flow using nondominated sorting multi objective gravitational search algorithm. Int J Electr Power Energy Syst 2014;62:323–34.
[8] Abido MA. Optimal power flow using Tabu search algorithm. Electr Power Compon Syst 2002;30(5):469–83.
[9] Roy PK, Ghoshal SP, Thakur SS. Constrained optimal power flow using craziness based particle swarm optimization considering valve point loading and prohibited operating zone. In: Proceedings of the international conference on power systems (ICPS'09). Kharagpur (India); 2009. p. 1–4.
[10] Roy PK, Ghoshal SP, Thakur SS. Multi-objective optimal power flow using biogeography based optimization. Electr Power Compon Syst 2010;38(12):1406–26.
[11] Roy PK, Ghoshal SP, Thakur SS. Biogeography based optimization for multi-constraints optimal power flow with emission and non-smooth cost function. Expert Syst Appl 2010;37(12):8221–8.
[12] Bhattacharya A, Chattopadhyay PK. Application of biogeography-based optimization to solve different optimal power flow problems. IET Gener Transm Distrib 2011;5(1):70–80.
[13] Hingorani NG. Power electronics in electrical utilities: role of power electronics in future power systems. Proc IEEE 1988;76(4):481–2.
[14] Basu M. Optimal power flow with FACTS devices using differential evolution. Int J Electr Power Energy Syst 2008;30(2):150–6.
[15] Basu M. Multi-objective optimal power flow with FACTS devices. Energy Convers Manage 2011;52(2):903–10.
[16] Chung TS, Li YK. A hybrid GA approach for OPF with consideration of FACTS devices. IEEE Power Eng Rev 2000;20(8):54–7.
[17] Ongsakul W, Bhasaputra P. Optimal power flow with FACTS devices by hybrid TS/SA approach. Int J Electr Power Energy Syst 2002;24(10):851–7.
[18] Belkacem M, Bouktir T, Srairi K, et al. Dynamic strategy based fast decomposed GA coordinated with FACTS devices to enhance the optimal power flow. Energy Convers Manage 2010;51(7):1370–80.
[19] Roy PK, Ghoshal SP, Thakur SS. Optimal power flow with TCSC and TCPS modeling using craziness and turbulent crazy particle swarm optimization. Int J Swarm Intel Res, IGI Global Pub 2010;1(3):34–50.
[20] Singh RP, Mukherjee V, Ghoshal SP. Particle swarm optimization with an aging leader and challengers algorithm for optimal power flow problem with FACTS devices. Int J Electr Power Energy Syst 2015;64:1185–96.
[21] Gandomi AH, Alavi AH. Krill herd: a new bio-inspired optimization algorithm. Commun in Nonlinear Sci Numer Simul 2012;17(12):4831–45.
[22] Wang G, Guo L, Wang H, et al. Incorporating mutation scheme into krill herd algorithm for global numerical optimization. Neural Comput Appl 2014;24(3):853–71.
[23] Bacanin N, Pelevic B, Tuba M. Krill herd (KH) algorithm for portfolio optimization. Math Comp Bus, Manuf Tour 39–44. ISBN: 978-960-474-332-2.
[24] Adhvaryyu PK, Chattopadhyay PK, Bhattachariya A. Application of bio-inspired krill herd algorithm to combined heat and power economic dispatch. In: Proceedings IEEE innovative smart grid technologies-Asia (ISGT Asia); 2014. p. 338–43.
[25] Gandomi AH, Alavi AH, Talatahari S. Structural optimization using krill herd algorithm. Chapter 15. In: Yang XS et al., editors. Swarm intelligence and bio-inspired computation: theory and applications. Elsevier; 2013. p. 335–49.
[26] Gandomi AH, Talatahari S, Tadbiri F, et al. Krill herd algorithm for optimum design of truss structures. Int J Bio-inspired Comput 2013;5(5):281–8.
[27] Wang G-G, Guo L, Gandomi AH, et al. Chaotic krill herd algorithm. Inf Sci 2014;274:17–34.
[28] Mukherjee A, Mukherjee V. Solution of optimal reactive power dispatch by chaotic krill herd algorithm. IET Gener Transm Distrib 2015;9(15):2351–62.
[29] Fattahi E, Bidar M, Kanan HR. Fuzzy krill herd optimization algorithm. In: IEEE first international conference on networks & soft computation (ICNSC); 2014. p. 423–26.
[30] Wang G, Gandomi AH, Alavi AH. Stud krill herd algorithm. Neurocomputing 2014;128:363–70.
[31] Mandal B, Roy PK, Mandal S. Economic load dispatch using krill herd algorithm. Int J Electr Power Energy Syst 2014;57:1–10.
[32] Tizhoosh HR. Opposition-based learning: a new scheme for machine intelligence. In: Proceedings of the international conference on computation intelligence on modelling control automation 2005 and international conference on intelligent agents. Web Tech Internet Commerce. p. 695–701.
[33] Wang H, Wu ZJ, Rahnamayan S, et al. Enhancing particle swarm optimization using generalized opposition-based learning. Inf Sci 2011;181(20):4699–714.
[34] Wang H, Liu Y, Zeng SY, et al. Opposition based particle swarm algorithm with Cauchy mutation. In: Proceedings of the IEEE congress on evolution computation (CEC 2007); 2007. p. 4750–6.
[35] Roy PK, Mandal D. Oppositional biogeography-based optimization for optimal power flow. Int J Power Energy Conv 2014;5(1):47–69.

[36] Zhang X, Rehtanz C, Pal B. Flexible AC transmission systems: modelling and control. Berlin: Springer; 2006.
[37] Shaw B, Ghoshal SP, Mukherjee V. Solution of combined economic and emission dispatch problem using hybrid craziness-based PSO with differential evolution. In: Proceedings of the IEEE symposium differential evolution (SDE-2011); 2011. p. 1–8.
[38] Shaw B, Mukherjee V, Ghoshal SP. A novel opposition-based gravitational search algorithm for combined economic and emission dispatch problems of power systems. Int J Electr Power Energy Syst 2012;35(1):21–33.
[39] Rahnamayan S, Tizhoosh HR, Salama MMA. Opposition versus randomness in soft computing techniques. Appl Soft Comput 2008;8(2):906–18.
[40] Rahnamayan S, Tizhoosh HR, Salama MMA. Opposition-based differential evolution for optimization of noisy problems. In: Proceedings of the IEEE congress on evolution computation (CEC 2006); 2006. p. 1865–72.
[41] Rahnamayan S, Tizhoosh HR, Salama MMA. Opposition-based differential evolution algorithms. In: Proceedings of the IEEE congress on evolution computation (CEC 2006); 2006. p. 2010–7.
[42] Rahnamayan S, Tizhoosh HR, Salama MMA. Opposition-based differential evolution. IEEE Trans Evol Comput 2008;12(1):64–79.
[43] Tizhoosh HR. Opposition-based reinforcement learning. J Adv Comput Intell Intell Inf 2006;10(4):578–85.
[44] Khalvati F, Tizhoosh HR, Aagaard MD. Opposition-based window memorization for morphological algorithms. In: Proceedings of the IEEE symposium on computational intelligence in image and signal processing. Honolulu (USA); 2007. p. 425–30.
[45] Al-Qunaieer FS, Tizhoosh HR, Rahnamayan S. Oppositional fuzzy image thresholding. In: Proceedings of the IEEE international conference on fuzzy systems. Barcelona (Spain); 2010. p. 1–7.
[46] Tizhoosh HR. Opposite fuzzy sets with applications in image processing. In: Proceedings of the joint 2009 international fuzzy systems association world congress and 2009 European society of fuzzy logic and technology conference. Lisbon (Portugal); 2009. p. 36–41.
[47] Malisia AR, Tizhoosh HR. Applying opposition-based ideas to the ant colony system. In: Proceedings IEEE swarm intelligence symposium. Honolulu (USA); 2007. p. 182–9.
[48] Montgomery J, Randall M. Anti-pheromone as a tool for better exploration of search space. In: Proceedings of the third international workshop on ant algorithms. Brussels (Belgium); 2002. p. 100–10.
[49] Haiping M, Xieyong R, Baogen J. Oppositional ant colony optimization algorithm and its application to fault monitoring. In: Proceedings of the 29th Chinese control conference (CCC); 2010. p. 3895–8.
[50] Lin ZY, Wang LL. A new opposition-based compact genetic algorithm with fluctuation. J Comput Inf Syst 2010;6(3):897–904.
[51] Ventresca M, Tizhoosh HR. Improving the convergence of backpropagation by opposite transfer functions. In: Proceedings of the international joint conference on neural networks (IJCNN'06). Vancouver (Canada); 2006. p. 4777–84.
[52] Ventresca M, Tizhoosh HR. Opposite transfer functions and backpropagation through time. In: Proceedings of the IEEE symposium on foundations of computational intelligence. Honolulu (USA); 2007. p. 570–7.
[53] Han L, He XS. A novel opposition-based particle swarm optimization for noisy problems. In: Proceedings of the third international conference on natural computation (ICNC 2007). Haikou (China); 2007. p. 624–9.
[54] Chatterjee A, Ghoshal SP, Mukherjee V. Solution of combined economic and emission dispatch problems of power systems by an opposition based harmony search algorithm. Int J Electr Power Energy Syst 2012;39(1):9–20.
[55] Bhattacharya A, Chattopadhyay PK. Solution of economic power dispatch problems using oppositional biogeography-based optimization. Electr Power Comp Syst 2010;38(10):1139–60.
[56] Ergezer M, Simon D, Du DW. Oppositional biogeography-based optimization. In: Proceedings of the IEEE International Conference on Systems, Man and Cybernetics (SMC 2009). San Antonio (USA); 2009. p. 1009–14.
[57] Saadat H. Power system analysis. Tata Mc-Graw-Hill; 2002.
[58] Zimmerman RD, Murillo-Sanchez CE, Gan D. MATPOWER: a matlab power system simulation package <http://www.pserc.cornell.edu/matpower/> [accessed on: 13 September 2014].
[59] The IEEE 57-bus test system <http://www.ee.washington.edu/research/pstca/pf57/pg_tca57bus.htm> [accessed on: 13 September 2014].